On singularities of solution of the elasticity system in a bounded domain with angular corner points

Yasir Nadeem Anjam*, [1,2] and Akhtar Ali [3]

[1]School of Mathematical Sciences, Shanghai Jiao Tong University, Shanghai 200240, P.R.China
[2]Department of Applied Sciences, National Textile University, Faisalabad 37610, Pakistan
[3]Department of Mathematics Government College University Faisalabad, 38000, Pakistan

Abstract: This paper aims to give a mathematically rigorous description of the corner singularities of the weak solutions for the plane linearized elasticity system in a bounded planar domain with angular corner points on the boundary. The qualitative properties of the solution including its regularity depend crucially on these corner points or such types of boundary conditions. In particular, the resulting expansion of the solutions of the underlying problem involves singular vector functions, inlines, depending on a certain parameter ξ_μ. We derive the transcendental equations for all ten possible cases of combinations of the boundary conditions generated by the basic four ones in classical elasticity proposing in the two natural directions of the boundary, i.e., tangential and normal direction, respectively, which depends on ξ_μ. So, a MATLAB program is developed whereby ξ_μ can be computed, and figures showing their distributions are presented. The leading singular exponents are computed for these combinations of the boundary conditions, wherein critical angles $\omega_{critical}$ are listed such that for interior angles $\omega < \omega_{critical}$ the H^2-regularity of solution can be guaranteed. Moreover, the characterization of stress singularities in terms of the inner angle of a corner point is studied, and the regularity results are given.
Keywords: Elasticity system; corner singularities; regularity; non-smooth domain.

1 Introduction

In the theory of elasticity, it is important to know the stress behavior in the neighborhood of reentrant corners and cracks for physical, theoretical, and numerical reasons. In fact, the solution can be supposed to be singular and this influences the structural strength of elastic materials. Also, the type of singularity has an impact on the qualitative behavior of failure of linear elasticity theory in such neighborhoods. Mathematical considerations, moreover, reveal that the usual boundary conditions have to be supplemented at corners to have well-formulated boundary value problems. The problems of the plane theory of linearized elasticity are stated that near the angular corner points or points where the types of boundary conditions change may cause stress singularities [16]. It means that the stresses can be unbounded on these points. The Lam*é* equations are generally used for two cases of equilibrium for elastic bodies. These cases are

*Corresponding Email: ynanjam@ntu.edu.pk

explicitly called the case of plane stress and the case of plane strain, which describes the deformation of the thin elastic plate under named the membrane loading [1, 4, 24, 30].

The eigenfunction expansion method has been used to analyze the two-dimensional (in-plane and out-of-plane) singular stress field at a thin plate with angular corners or finite opening cracks [33]. Dempsey and Sinclair [10] have introduced a new form of Airy stress function to investigate the stress singularities of isotropic elastic plates in extension. The mathematical derivation for the static bending problem of isotropic sectorial plates that contain stress singularities at the vertex of the plates owing to geometry and boundary conditions is described in [5]. In [15], the Mellin transform has been used to examine the stress singularities in a two-material wedge. [11] has employed a complex potential approach to analyze the form of eigenvector solutions for a general corner or an opening crack problem. Sinclair [28] has studied the Logarithmic stress singularities in a problem of plates in extension with various boundary conditions.

Generally, the questions of corner singularities are examined for three types of boundary conditions, such as Dirichlet, Neumann, or the mixed (Dirichlet-Neumann and vice versa) boundary conditions for bounded plane domains with corners [12, 31, 34]. [29] has used the Airy stress function to analyze the stress singularities with the combinations of the three of the four boundary conditions (Dirichlet, Neumann, Soft clamped), but no singular expansion or the regularity of the solutions was considered. Seweryn and Molski [27] have studied the elastic stress singularities and the generalized formulations of the stress intensity factors near the angular corners with different boundary conditions but again the regularity of solutions is not studied. The qualitative properties of solution of the elasticity system including its regularity in non-smooth domains with corner points and cracks with the applications of classical and weighted Sobolev spaces were thoroughly studied in [21, 26]. Rössle and Sändig [25] have used these results to investigate the geometric singularities and regularity of the Reissner Mindlin plate model. Brown and Mitrea [6] have considered the mixed problem for the Lam*é* system in a class of Lipschitz domains. Ott and Brown [23] have considered the Lam*é* system in a bounded Lipschitz domain to determine the existence of a unique solution when the data is taken from Hardy spaces and Hardy-Sobolev spaces. Recently, the two-dimensional elasticity problem is considered to investigate the existence and uniqueness analysis through the single-layer potential approach [20].

The rest of this paper is as follows. In Section 2, the classical formulation of the elasticity system and as a weak problem is presented. The corresponding theorem which expresses the singular expansion of the solution of the elasticity problem near the angular corner point is stated. In Section 3, after localizing the problem at each angular corner point of the domain, applying the method of ansatzs leads to a boundary eigenvalue problem with the parameter. The transcendental equations illustrating the corner singularity exponents for various possible cases of the combinations of the boundary conditions are derived, and their distributions are shown graphically in Section 3.2. In Table 1 critical angles $\omega_{critical}$ are listed such that for interior angles $\omega < \omega_{critical}$ the H^2-regularity of solution can be guaranteed. The concluding remarks on the regularity of solutions to the considered problem are given in Section 4.

2 The Elasticity System

2.1 Classical Formulation

Let $\Omega \subset \mathbb{R}^2$ be a two-dimensional bounded and connected domain, whose boundary $\partial\Omega = \Gamma$ comprises the angular corner points, the points at which the types of boundary conditions change. Let $\mathcal{M}$ denote the set of these boundary points which consists of $\mathcal{M} = \{P_1, ..., P_N\} \subset \partial\Omega$. Let $\omega_i, i = 1, 2, ..., N$ denote the corresponding interior angle made by the open edges Γ_{i-1} and Γ_i.

Let $\mathbf{u} = (u_1, u_2)^T$ be the displacement vector field with the cartesian components u_1, u_2, where the linearized strain tensor $\epsilon(\mathbf{u})$ is defined by

$$\epsilon_{ij}(\mathbf{u}) = \frac{1}{2}\Big(\frac{\partial u_i}{\partial x_j} + \frac{\partial u_j}{\partial x_i}\Big), \quad \text{for } i,\, j = 1, 2. \tag{2.1}$$

The corresponding linearized stress tensor $\sigma(\mathbf{u})$ is given according to Hooke's law by using the Lam*é* coefficients μ and Λ (μ and Λ are always assumed to be positive):

$$\sigma_{ij}(\mathbf{u}) = \mu\Big(\frac{\partial u_i}{\partial x_j} + \frac{\partial u_j}{\partial x_i}\Big) + \Lambda\big(\operatorname{div}(\mathbf{u})\big)\delta_{ij}, \quad \text{for } i,\, j = 1, 2, \tag{2.2}$$

where $\delta_{i\,j}$ is the Kronecker symbol, $\operatorname{div}\mathbf{u} = \partial_1 u_1 + \partial_2 u_2$, and ∂_i, $i = 1, 2$ means differentiation with respect to x_i. To consider the possible boundary conditions on the boundary Γ, we assume in the consequence the four canonical choices which describe basic ones in classical elasticity proposing in the two natural directions of the boundary, i.e., tangential and normal direction, respectively, and are asserted in [19, 25]. These are such type of conditions that can be imposed in the variational formulation of the underlying problem. In the plane stress case, when the thickness of the plate tends to zero then these conditions can be considered as two-dimensional limit boundary conditions [9]. For the formulation, we suppose that the boundary Γ is composed as $\Gamma = \Gamma_a \cup \Gamma_b \cup \Gamma_c \cup \Gamma_d$, where Γ_a, Γ_b, Γ_c, and Γ_d are the disjoint parts of the boundary Γ, and maybe each of them is empty.

Let us consider the linear plane strain elasticity problem on a domain Ω:

$$\mu\Delta\mathbf{u} + (\mu + \Lambda)\,\mathbf{grad}\,(\operatorname{div}\mathbf{u}) = -\mathbf{f} \quad \text{in} \quad \Omega, \tag{2.3}$$

with boundary conditions

$$\mathbf{u} = 0, \quad \text{on} \quad \Gamma_a, \tag{2.4}$$

$$u_n = 0, \quad \sigma_{n,\tau} = 0, \quad \text{on} \quad \Gamma_b, \tag{2.5}$$

$$\sigma_{n,n} = 0, \quad u_\tau = 0, \quad \text{on} \quad \Gamma_c, \tag{2.6}$$

$$\sigma(\mathbf{u})\,\mathbf{n} = 0, \quad \text{on} \quad \Gamma_d, \tag{2.7}$$

where $\mathbf{f} = (f_1, f_2)^T$ is the force density applied on the body Ω, $\mathbf{grad} = (\partial_1, \partial_2)^T$, Δ is the Laplacian, and $\mathbf{n}$ is the exterior normal to Γ. Let $u_n = \mathbf{u}\cdot\mathbf{n}$ is the normal components of the vector field $\mathbf{u}$ on the boundary, i.e., $u_n = u_1 n_1 + u_2 n_2$, while u_τ is the tangential components of the vector $\mathbf{u}$, i.e., $u_\tau = u_1 n_2 - u_2 n_1$. Let $\sigma(\mathbf{u})\,\mathbf{n}$ describes the outward traction field at a point on Γ. The similar notations as above can be applied to describe its normal and tangential components. For more information about the boundary conditions, we refer to [Chapter 4, 18] and [25].

Moreover, the boundary conditions (2.4)-(2.7) represents the hard clamped (HC), soft clamped (SC), simply supported (SS), and stress-free (SF) boundary conditions. The formulation (2.3) is used for the case of plane strain, whereas the Lam*é* operator for the case of plane stress state can simply be obtained to replace the Lam*é* coefficients Λ by $\widetilde{\Lambda} = \dfrac{2\mu\Lambda}{\Lambda + 2\mu}$ from [2].

Now, using the differential operator L and the boundary operator B, one can write shortly (2.3)-(2.7) as

$$\begin{cases} L\,\mathbf{u} = -\mathbf{f} \quad \text{in} \quad \Omega, \\ B\,\mathbf{u} = 0 \quad \text{on} \quad \Gamma. \end{cases} \tag{2.8}$$

2.2 Weak Formulation

In this subsection, the weak formulation of the problem (2.8) is given. Let

$$W(\Omega) = \Big\{ \mathbf{u} \in H^1(\Omega)^2 \big|\, \mathbf{u} \,\text{satisfies the essential boundary conditions on } \Gamma \Big\}, \tag{2.9}$$

be the set of admissible displacement fields, containing fields with finite energy sustaining the geometrical constraints on the boundary Γ. These assumptions are satisfied if the meas $\Gamma_a > 0$. Let $\mathcal{N}$ denote the set of the rigid movements in $W(\Omega)$, i.e.,

$$\mathcal{N} = \Big\{ \mathbf{v}(\mathrm{x}) = \begin{pmatrix} c_1 - c x_2 \\ c_2 + c x_1 \end{pmatrix} \;\Big|\; \mathbf{v}(\mathrm{x}) \in W(\Omega),\, c,\, c_1,\, c_2 \in \mathbb{R} \Big\}. \tag{2.10}$$

If for example, the boundary piece where the hard clamped boundary conditions are levied has a positive measure, then $\mathcal{N} = \emptyset$. Instead, if the stress-free boundary conditions are levied on the whole Γ, which means that $\Gamma_d = \Gamma$, then the set $\mathcal{N}$ is three -dimensional and contains all rigid motions.

Seek $\mathbf{u} \in W(\Omega)$, such that

$$a\big(\mathbf{u}, \mathbf{v}\big) = \mathbf{f}\,(\mathbf{v}), \;\text{ for every } \mathbf{v} \in W(\Omega), \tag{2.11}$$

where

$$a\big(\mathbf{u}, \mathbf{v}\big) = \int_\Omega \sum_{i,j=1,2} \sigma_{ij}(\mathbf{u})\, \epsilon_{ij}(\mathbf{v})\, d\mathrm{x} \quad \text{and} \quad \mathbf{f}\,(\mathbf{v}) = \int_\Omega \mathbf{f}.\,\mathbf{v}\, d\mathrm{x}.$$

Employing a form of the Korn inequality with the considered boundary conditions gives the coercivity of the bilinear form $a\big(.,.\big)$ in (2.11) on the space

$$\mathcal{U}(\Omega) = \Big\{ \mathbf{u}(\mathrm{x}) \in W(\Omega) \Big| : \int_\Omega \mathbf{u}.\,\mathbf{v}\, d\mathrm{x} = 0, \quad \forall \mathbf{v} \in \mathcal{N} \Big\}. \tag{2.12}$$

Due to this Korn inequality with boundary conditions, the Lax-Milgram lemma is relevant and consequently, a unique weak solution $\mathbf{u} \in \mathcal{U}(\Omega)$ of the variational problem (2.11) exists if the right-hand side fulfills the following compatibility condition

$$\int_\Omega \mathbf{f}.\,\mathbf{v}\, d\mathrm{x} = 0, \;\text{ for every } \mathbf{v} \in \mathcal{N}. \tag{2.13}$$

The understanding of the eigenvalues and corresponding eigenfunctions are crucial to describe the behavior of solution $\mathbf{u} \in \mathcal{U}(\Omega)$ of the problem (2.11) in the neighborhood of the angular corner points. The following theorem states this fact which is a classical result.

Theorem 2.1. *[8, 17]* (**Expansion theorem**): Given $\mathbf{f} \in L^p(\Omega)^2$, $1 \leq p < \infty$, let $\mathbf{u} \in \mathcal{U}(\Omega)$ be the unique weak solution of the problem (2.11) and P is an isolated angular corner point of Γ. If $\xi_1, \xi_2, ..., \xi_N$ are the eigenvalues of the operator $\hat{\mathcal{V}}(\xi)$, then the solution $\mathbf{u}$ admits the following expansion in a neighborhood $\eta(P)$ of P, i.e.,

$$\mathbf{u} = \chi(r) \left[\sum_{\mu=1}^{N} \sum_{\rho=1}^{I_\mu} \sum_{\kappa=0}^{\kappa_{\mu\rho}-1} c_{\mu,\,\rho,\,\kappa}\, \mathbf{S}_{\mu,\,\rho,\,\kappa}(r,\,\theta) \right] + \mathbf{w}_{reg}(r,\,\theta), \tag{2.14}$$

with $\mathbf{w}_{reg}(r,\,\theta) \in W^{2,\,p}\big(\eta(P)\big)$ and χ is the cut-off function (3.1). Here, N be the number of all eigenvalues of the operator pencil $\hat{\mathcal{V}}(\xi)$ in the strip $\mathcal{R}e(\xi_\mu) \in (0, 2 - \frac{2}{p})$, the constants $c_{\mu,\,\rho,\,\kappa}$ depend on the data and the singular functions, $I_\mu = \dim \operatorname{Ker} \hat{\mathcal{V}}(\xi_\mu)$, $\kappa_{\mu\rho}$ is the length of the Jordan chains of $\hat{\mathcal{V}}(\xi_\mu)$ and the corresponding singular functions are given by

$$\mathbf{S}_{\mu,\,\rho,\,\kappa}(r,\,\theta) = r^{\xi_\mu} \sum_{j=0}^{\kappa} \frac{(\log r)^j}{j!}\, \Phi_\mu^{\rho,\,\kappa-j}(\theta), \tag{2.15}$$

where $\Phi_\mu^{\rho,\,\kappa-j}(\theta)$ is a canonical system of Jordan chains of $\hat{\mathcal{V}}(\xi)$ respecting ξ_μ.

It is noted from (2.14) and (2.15) that the eigenvalues $\xi_\mu = 0$ do not yield singularities in the development of the solution in the neighborhood $\eta(P)$.

Remarks 2.1. It is observed that the knowledge of the singular exponents ξ_μ in (2.15) which is known as eigenvalues leads to determine the qualitative properties of the solution including regularity of the underlying problem. Since they generate the singular functions as a power of r. It is observed that if $\mathcal{R}e\,(\xi_\mu) \geq 1$, then the general solution defined in (2.14) is regular and belongs to $W^{2,2}(\Omega)^2$. The case $\mathcal{R}e\,(\xi_\mu) = 0$ represents the translation which is regular. Normally, the terms with $\mathcal{R}e\,(\xi_\mu) < 1$ are called the singular terms since they produce the unbounded stresses. The logarithmic terms occur only if ξ_μ has the algebraic multiplicity greater than one. Furthermore, the generalized eigenvalues are dependent on the values of the apex angle ω_0.

It is observed from (2.14) and (2.15) that the resulting expansion contains singular vector functions, which in turn relies on the values of parameter ξ_μ. Furthermore, the knowledge of the values of parameter ξ_μ leads to determine the regularity and singularity properties of the solution of the given problem. So to obtain the results, the following steps are followed.

1. Localize the elasticity problem (2.8) in the neighborhood of an angular corner point and then consider the problem (2.8) in an infinite wedge. The problem (2.8) is written in local polar coordinates $(r,\,\theta)$, and applying the method of ansatzs leads to a boundary eigenvalue problem with the parameter.

2. We derive the transcendental equations for this parametric boundary eigenvalue problem for various possible combinations of the boundary conditions with the aid of the determinant method. Analytically, it is much difficult to compute the values of ξ_μ, which are explicitly called the generalized eigenvalues of the given problem.

3. So with the aid of the Newton method from computation, a MATLAB program is developed to compute the eigenvalues $\mathcal{R}e\,(\xi_\mu)$, and the figures showing their distributions are given.

4. Finally, we determine the leading singular exponents for all the possible combinations of the boundary conditions, and the critical angles $\omega_{critical}$ are listed which helps to determine the regularity results.

3 The Elasticity System in an Infinite Wedge

3.1 Localization

We consider a weak solution $\mathbf{u} \in \mathcal{U}(\Omega) \subset H^1(\Omega)^2$ to (2.11), assuming that $\mathbf{f} \in L^2(\Omega)^2$. Generally, it is recognized that the solution $\mathbf{u}$ does not belongs to $H^2(\Omega)^2$ owing to the geometrical singularities of the boundary, for instance, the angular corner points or points upon which the types of boundary conditions change. Consider the point $P_N \in \{P_i\}$ as origin with the interior angle $\omega_N = \omega_0 \in (0, 2\pi)$, and an appropriate infinite differentiable cut-off function $\chi(|\mathrm{x}|) = \chi(r)$ depending on the distance r from the point P_N is defined as

$$\chi(r) = \begin{cases} 1 & \text{for} \quad 0 < r < \frac{\delta}{2}, \\ 0 & \text{for} \quad r > \delta. \end{cases} \tag{3.1}$$

We multiply on the both-sides of (2.8) by the smooth cut-off function χ, then substitute $\mathbf{v} = \chi\mathbf{u}$ in (2.8). The derivatives are considered in the distribution sense. Thus, the boundary value problem (2.8) is set on the infinite wedge

$$\mathcal{W} = \Big\{ \mathrm{x} = (x_1, x_2) \in \mathbb{R}^2 \,\Big|\, (r,\, \theta) : 0 \le r < \infty,\, -\frac{\omega_0}{2} < \theta < \frac{\omega_0}{2} \Big\},$$

and coincides with the original problem near the point P_N. Therefore, the problem (2.8) becomes

$$\begin{cases} L\,\mathbf{v} = & -\mathbf{F}(\mathrm{x}) \quad \text{in} \quad \mathcal{W}, \\ B^{\pm}\,\mathbf{v} = & 0 \quad \text{on} \quad \Gamma^{\pm}, \end{cases} \tag{3.2}$$

where $\mathbf{F} = (F_1, F_2)$ and the function F_1 is as follows

$$F_1 = \begin{cases} \mu\big(\chi\Delta u_1 + u_1\Delta\chi + 2\frac{\partial\chi}{\partial x_1}\,\frac{\partial u_1}{\partial x_1} + 2\frac{\partial\chi}{\partial x_2}\,\frac{\partial u_1}{\partial x_2}\big) + (\mu+\Lambda)\Big(\chi\,\frac{\partial^2 u_1}{\partial {x_1}^2} + \frac{\partial^2 u_2}{\partial x_1\,\partial x_2} \\ +u_1\frac{\partial^2\chi}{\partial {x_1}^2} + 2\frac{\partial u_1}{\partial x_1}\,\frac{\partial\chi}{\partial x_1} + u_2\frac{\partial^2\chi}{\partial x_1\,\partial x_2} + \frac{\partial u_2}{\partial x_2}\frac{\partial\chi}{\partial x_1} + \frac{\partial\chi}{\partial x_2}\frac{\partial u_2}{\partial x_1}\Big). \end{cases}$$

F_2 has the similar form. The behavior of $\mathbf{v}$ near the point P_N illustrates the regularity of the solution $\mathbf{u}$ in the neighborhood of the point P_N. It is stated that just only one condition is prescribed on the whole Γ^- and possibly another condition is prescribed on the whole Γ^+.

For the regularity analysis of the boundary value problem (3.2), we rewrite the operators in polar coordinates as follows:

$$\begin{aligned} &\mu\Big(\frac{\partial^2 v_r}{\partial r^2} + \frac{1}{r}\frac{\partial v_r}{\partial r} + \frac{1}{r^2}\frac{\partial^2 v_r}{\partial\theta^2} - \frac{v_r}{r^2} - \frac{2}{r^2}\frac{\partial v_\theta}{\partial\theta}\Big) + (\Lambda+\mu)\frac{\partial}{\partial r}\Big(\frac{\partial v_r}{\partial r} + \frac{1}{r}v_r + \frac{1}{r}\frac{\partial v_\theta}{\partial\theta}\Big) = -F_r, \\ &\mu\Big(\frac{\partial^2 v_\theta}{\partial r^2} + \frac{1}{r}\frac{\partial v_\theta}{\partial r} + \frac{1}{r^2}\frac{\partial^2 v_\theta}{\partial\theta^2} - \frac{v_\theta}{r^2} + \frac{2}{r^2}\frac{\partial v_r}{\partial\theta}\Big) + (\Lambda+\mu)\frac{1}{r}\frac{\partial}{\partial\theta}\Big(\frac{\partial v_r}{\partial r} + \frac{1}{r}v_r + \frac{1}{r}\frac{\partial v_\theta}{\partial\theta}\Big) = -F_\theta, \end{aligned} \tag{3.3}$$

where (v_r, v_θ), (F_r, F_θ) are the polar components of the displacement vector field $\overline{\mathbf{v}}$, and $\overline{\mathbf{F}}$, respectively. Hence

$$\overline{\mathbf{v}} = \begin{pmatrix} v_r \\ v_\theta \end{pmatrix} = A \begin{pmatrix} v_1 \\ v_2 \end{pmatrix}, \ \overline{\mathbf{F}} = \begin{pmatrix} F_r \\ F_\theta \end{pmatrix} = A \begin{pmatrix} F_1 \\ F_2 \end{pmatrix}, \ A = \begin{pmatrix} \cos\theta & \sin\theta \\ -\sin\theta & \cos\theta \end{pmatrix}.$$

The components of the stress tensor in polar coordinates are described as

$$\sigma_{rr} = 2\mu \frac{\partial v_r}{\partial r} + \Lambda\big(\frac{\partial v_r}{\partial r} + \frac{v_r}{r} + \frac{1}{r}\frac{\partial v_\theta}{\partial \theta}\big), \tag{3.4}$$

$$\sigma_{\theta\theta} = 2\mu\big(\frac{1}{r}\frac{\partial v_\theta}{\partial \theta} + \frac{v_r}{r}\big) + \Lambda\big(\frac{\partial v_r}{\partial r} + \frac{v_r}{r} + \frac{1}{r}\frac{\partial v_\theta}{\partial \theta}\big), \tag{3.5}$$

$$\sigma_{r\theta} = \sigma_{\theta r} = \mu\big(\frac{1}{r}\frac{\partial v_r}{\partial \theta} + \frac{\partial v_\theta}{\partial r} - \frac{v_\theta}{r}\big). \tag{3.6}$$

We seek the solutions to the considered problem under the form

$$v_r(r,\, \theta) = r^\xi \hat{v}_r(\theta), \quad v_\theta(r,\, \theta) = r^\xi \hat{v}_\theta(\theta), \tag{3.7}$$

where $\xi \in \mathbb{C}$ is a complex number.

Using (3.7), the problem (3.3) emerges an ordinary differential system which depends analytically on the complex parameter ξ and holds on the interval $I = \theta \in \big(-\frac{\omega_0}{2},\, \frac{\omega_0}{2}\big)$. Thus the transformed form of the problem (3.3) is given by

$$\begin{aligned} \mu\frac{d^2\hat{v}_r}{d\theta^2} + (2\mu+\Lambda)(\xi^2-1)\hat{v}_r + \Big[-(\Lambda+3\mu) + (\mu+\Lambda)\xi\Big]\frac{d\hat{v}_\theta}{d\theta} &= -\hat{F}_r, \\ (2\mu+\Lambda)\frac{d^2\hat{v}_\theta}{d\theta^2} + \Big[(\Lambda+3\mu) + (\mu+\Lambda)\xi\Big]\frac{d\hat{v}_\theta}{d\theta} + \mu(\xi^2-1)\hat{v}_\theta &= -\hat{F}_\theta, \end{aligned} \tag{3.8}$$

whereas the transformed form of the Neumann boundary conditions emerges as

$$\hat{\sigma}_{r\theta} = \mu\big(\frac{d\hat{v}_r}{d\theta} + (\xi-1)\hat{v}_\theta\big) \ \text{ and } \ \hat{\sigma}_{\theta\theta} = (2\mu+\Lambda)\frac{d\hat{v}_\theta}{d\theta} + \big(2\mu + (\xi+1)\Lambda\big)\hat{v}_r. \tag{3.9}$$

Let $\hat{L}(\xi)$ denote the matrix differential operator analogous to the system (3.8). Analogously, the operator $\hat{B}_{[.\,.]}(\xi)$ is used to characterize the general transformed form of the matrix boundary operators for various combinations of the boundary conditions (2.4)-(2.7). Accordingly, the operator pencil $\hat{\mathcal{V}}(\xi)$ for a generalized eigenvalue problem can be written as

$$\hat{\mathcal{V}}(\xi) = \Big[\hat{L}(\xi),\, \big\{\hat{B}_{[.\,.]}(\xi)\big\}\Big]. \tag{3.10}$$

Thus, the operator $\hat{\mathcal{V}}(\xi)$ maps $W^{2,2}(I)^2$ into $L^2(I)^2 \times \mathbb{C}^2 \times \mathbb{C}^2$. Let $\hat{\mathcal{V}}(\xi)(\theta,\, \xi) = 0$ is used to describe a generalized eigenvalue problem and the solvability of such type of problems is discussed in [17, 32]. The operator $\hat{\mathcal{V}}(\xi)$ is an isomorphism for all $\xi \in \mathbb{C}$ apart from some isolated points (known as the eigenvalues of $\hat{\mathcal{V}}(\xi)$). So, the resolvent $\mathcal{R}(\xi) = \big[\hat{\mathcal{V}}(\xi)\big]^{-1}$ is an operator-valued, meromorphic function of ξ has poles of finite multiplicity. The eigenvalues of the operator $\hat{\mathcal{V}}(\xi)$ are obtained with the determinant method, this means that the nontrivial solution of the generalized eigenvalue problem leads to a transcendental equation whose zeros are the eigenvalues of $\hat{\mathcal{V}}(\xi)$.

The definition of the eigenvalues ξ_μ (whereas the subscript μ is generally used to refer to the multiple eigenvalues) and the corresponding eigenfunctions are described in the following definition.

Definition 3.1. *A complex number $\xi = \xi_0$ is known as eigenvalue of $\hat{\mathcal{V}}(\xi)$ if there exists a nontrivial solution i.e., $\hat{u}(.,\xi_0) \neq 0$, which is holomorphic at ξ_0, such that $\hat{\mathcal{V}}(\xi_0)\,\hat{u}(\theta,\xi_0) = 0$. $\hat{u}(\theta,\xi_0)$ is called an eigenfunction of $\hat{\mathcal{V}}(\xi_0)$ corresponding to the eigenvalue ξ_0. The set of fields $\{\hat{u}_0(\theta,\xi_0),\, \hat{u}_{0,1}(\theta,\xi_0), ...,\, \hat{u}_{0,s}(\theta,\xi_0)\}$ with $\hat{u}_{0,0} = \hat{u}_0$ is said to be a Jordan chain corresponding to the eigenvalue ξ_0, if the equation*

$$\sum_{q=0}^{m} \frac{1}{q!} \big(\frac{\partial}{\partial \xi}\big)^q \hat{\mathcal{V}}(\xi)\, \hat{u}_{0,m-q}(\theta,\xi)\Big|_{\xi=\xi_0} = 0 \quad \textit{for} \quad m = 1, 2, ..., s,$$

is satisfied. The number $s+1$ is called the length of the Jordan chain.

3.2 Distributions of the Eigenvalues

In this section, the general solutions of the homogenous system (3.8) are given. The transcendental functions whose roots are the eigenvalues of the operator $\hat{\mathcal{V}}(\xi)$ for all the possible cases of the combinations of the boundary conditions (2.4)-(2.7) are derived. Moreover, the distributions of the generalized eigenvalues are computed numerically.

The fundamental solution of the homogenous parametric dependent system (3.8) for the case of $\xi \neq 0$ is given by

$$\begin{pmatrix} \hat{v}_r \\ \hat{v}_\theta \end{pmatrix} = \begin{cases} B_1 \begin{pmatrix} \sin[(\xi+1)\theta] \\ \cos[(\xi+1)\theta] \end{pmatrix} + B_2 \begin{pmatrix} \cos[(\xi+1)\theta] \\ -\sin[(\xi+1)\theta] \end{pmatrix} \\ +B_3 \begin{pmatrix} \big(3\mu+\Lambda-\xi(\mu+\Lambda)\big)\, \cos[(1-\xi)\theta] \\ -\big(3\mu+\Lambda+\xi(\mu+\Lambda)\big)\, \sin[(1-\xi)\theta] \end{pmatrix} \\ +B_4 \begin{pmatrix} \big(3\mu+\Lambda-\xi(\mu+\Lambda)\big)\, \sin[(1-\xi)\theta] \\ \big(3\mu+\Lambda+\xi(\mu+\Lambda)\big)\, \cos[(1-\xi)\theta] \end{pmatrix}, \end{cases} \tag{3.11}$$

where $B_i \in \mathbb{R}$, $i = 1, 2, 3, 4$. For the case of $\xi = 0$, the general solution of the homogenous system (3.8) has the following form

$$\begin{pmatrix} \hat{v}_r \\ \hat{v}_\theta \end{pmatrix} = \begin{cases} B_1 \begin{pmatrix} \sin\theta \\ \cos\theta \end{pmatrix} + B_2 \begin{pmatrix} \cos\theta \\ -\sin\theta \end{pmatrix} \\ +B_3 \begin{pmatrix} -\big(3\mu+\Lambda\big)\,\theta\, \cos\theta + \mu\, \sin\theta \\ \big(3\mu+\Lambda\big)\,\theta\, \sin\theta + \big(2\mu+\Lambda\big)\, \cos\theta \end{pmatrix} \\ +B_4 \begin{pmatrix} \big(3\mu+\Lambda\big)\,\theta\, \sin\theta + \mu\, \cos\theta \\ \big(3\mu+\Lambda\big)\,\theta\, \cos\theta - \big(2\mu+\Lambda\big)\, \sin\theta \end{pmatrix}. \end{cases} \tag{3.12}$$

The coefficients $\mathbf{B} = (B_1, B_2, B_3, B_4)^T$ are determined according to the types of boundary conditions. Analogously, the tractions $\big(\hat{\sigma}_{r\theta}, \hat{\sigma}_{\theta\theta}\big)$ in (3.9) for the cases of $\xi \neq 0$ and $\xi = 0$ can be obtained by using (3.11) and (3.12).

To evaluate the eigenvalues and corresponding eigenfunctions of the elasticity system, the solution (3.11) with various possible combinations of the boundary conditions is considered to obtain a system of four linear homogeneous equations with our unknowns B_1, B_2, B_3, and B_4. The resulting matrix of coefficients of these equations depends on the complex parameter ξ, and a nontrivial solution exists if and only if the determinant of the resulting matrix of coefficients vanishes. Furthermore, it produces the transcendental equations whose roots are the eigenvalues, namely, ξ_μ for $\mu = 1, ...N$.

Moreover, for the case of plane strain, we consider the following relations between the Lam*é* coefficients μ, Λ and the Poisson's ratio $\nu = \frac{\Lambda}{2(\Lambda+\mu)}$, i.e.,

$$\frac{(\Lambda+3\mu)}{\Lambda+\mu} = 3-4\nu, \quad \frac{(\Lambda+2\mu)}{\mu} = \frac{2(1-\nu)}{1-2\nu}, \quad \text{and} \quad \frac{(\Lambda+3\mu)}{\mu} = \frac{3-4\nu}{1-2\nu}.$$

On the other hand, for the case of plane stress, the Poisson's ration ν has to be replaced by $\widetilde{\nu} = \frac{\nu}{(1+\nu)}$.

To compute the transcendental equations for different possible cases of the combinations of the boundary conditions, we proceed as follows.

Case 1: Hard clamped- Hard clamped boundary conditions (HC-HC)

It means that the hard clamped boundary conditions are given on both sides of the angular corner point. The determinant method is used to obtain a system of linear homogeneous equations. A non-trivial solution exists if the determinant $D_{HC-HC}(\xi)$ of the corresponding system of the matrix of coefficients vanishes. So, the obtained characteristic equation from (3.11) and (2.4) for the plane strain condition is given by

$$D_{HC-HC}(\xi) = \sin^2(\xi\omega_0) - \xi^2\Big(\frac{1}{3-4\nu}\Big)^2 \sin^2(\omega_0). \tag{3.13}$$

The roots of the equation (3.13) are the eigenvalues of the operator $\hat{\mathcal{V}}_{HC-HC}(\xi) = \big[\hat{L}(\xi), \{\hat{B}_{[HC-HC]}(\xi)\}\big]$.

The dispersal of zeros of equation (3.13) with $\mathcal{R}e(\xi) \in [0,4]$ and $\omega_0 \in (0, 2\pi)$ is shown in Figures 1a-3 for Poisson's ratios $\nu = 0.0, 0.29, 0.33, 0.41$, and 0.5. It ought to be observed that the singularity of the stress field arises only for the real value of the exponent ξ $\big(\mathcal{R}e\,(\xi) \in (0,1)$ and $\mathrm{Im}\,(\xi) = 0\big)$, which corresponds to $\omega_0 > \pi$. In all the subsequent graphs, the black lines reveal the real eigenvalues, while the red lines reveal the real parts of the conjugate pair of complex eigenvalues.

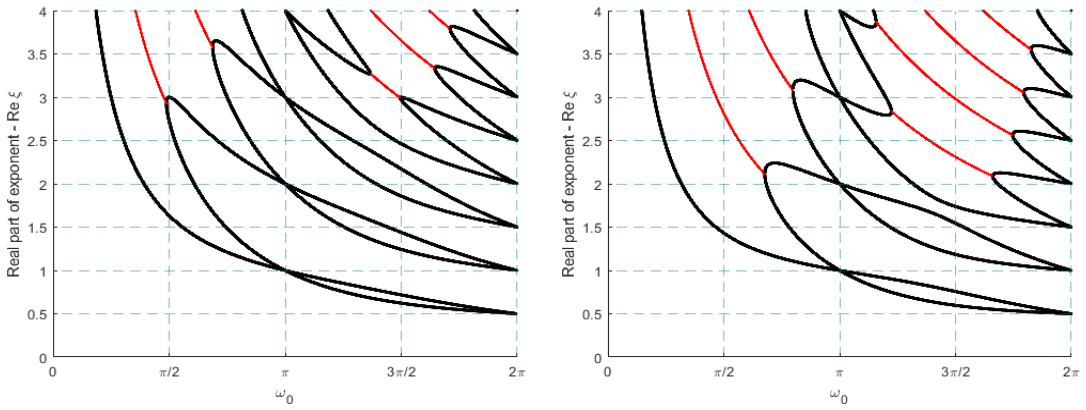

(a) Eigenvalues for HC-HC conditions for $\nu = 0.0$.

(b) Eigenvalues for HC-HC conditions for $\nu = 0.29$ (plane stress).

Figure 1: Distribution of the eigenvalues for HC-HC conditions for $\nu = 0.0$ and $\nu = 0.29$ (plane stress).

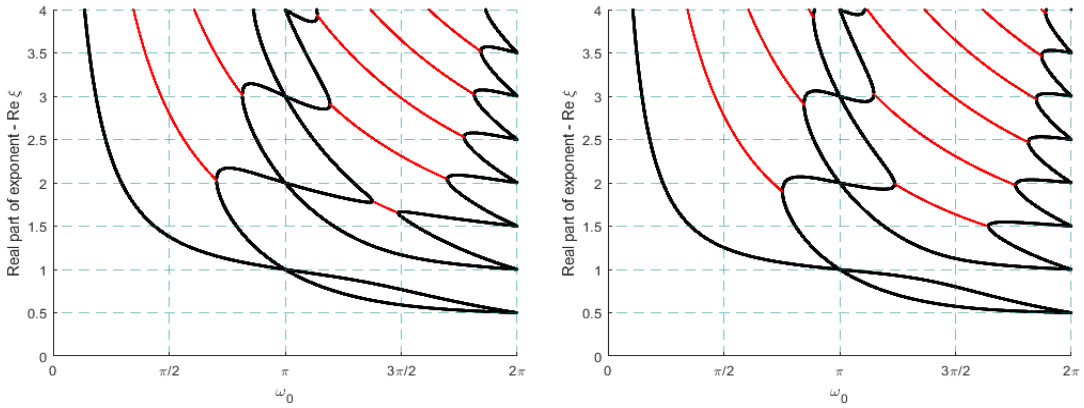

(a) Eigenvalues for HC-HC conditions for $\nu = 0.33$.

(b) Eigenvalues for HC-HC conditions for $\nu = 0.41$.

Figure 2: Distribution of the eigenvalues for HC-HC conditions for $\nu = 0.33$ and $\nu = 0.41$.

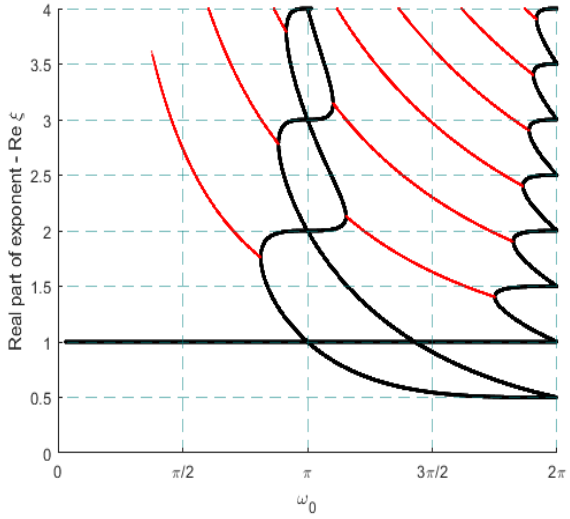

Figure 3: Distribution of the eigenvalues for HC-HC conditions for $\nu = 0.5$.

Case 2: Stress free- Stress free boundary conditions (SF-SF)

It means that the stress free boundary conditions are given on both sides of the angular corner point. So, the obtained characteristic equation for this case is

$$D_{SF-SF}(\alpha) = \sin^2(\xi\omega_0) - \xi^2 \sin^2(\omega_0). \tag{3.14}$$

The numerical solutions to equation (3.14) are shown in Figure 4 with $\mathcal{R}e(\xi) \in [0, 4]$ and $\omega_0 \in (0, 2\pi)$. Now, we give the results for the eigenvalues of the algebraic equation (3.14), and the others will be treated analogously. The singular exponents are attained by finding the roots of (3.14). Ordering these solutions with the non-decreasing real part, a non-decreasing sequence of numbers $\xi_\mu, \mu = 1, 2, ...N$ is obtained. The number s_μ is defined by

$$s_\mu = \mathcal{R}e\,(\xi_\mu) + 1,$$

which is known as the order of the regularity of the solution space and depends on the corner singularity. More information about the numbers ξ_μ can be found in [18]. Furthermore, the non-convex and convex cases are discussed separately regarding the values of apex angle ω_0.

Case I. For the non-convex case, that is $\omega_0 \in (\pi,\, 2\pi)$, the first 3 leading eigenvalues ξ_μ, $\mu = 1, 2, 3$ are real and the properties

$$\frac{1}{2} < \xi_1 < \frac{\pi}{\omega_0} < \xi_2 = 1 < \xi_3 < \frac{2\pi}{\omega_0}, \qquad \omega_0 \in (\pi, \omega^*], \tag{3.15}$$

$$\frac{1}{2} < \xi_1 < \frac{\pi}{\omega_0} < \xi_2 < \xi_3 = 1 < \frac{2\pi}{\omega_0}, \qquad \omega_0 \in (\omega^*, 2\pi), \tag{3.16}$$

hold. In particular, $\omega^* \approx 1.4303\pi$ is the unique solution of the equation $\tan\omega - \omega = 0$ in the interval $\omega \in [0, 2\pi)$. It can be seen that for an angle $\omega_0 \in (\omega^*, 2\pi)$, there are two eigenvalues ξ_1, ξ_2 less than 1.

Case II. For the convex case, that is $\omega_0 \in (0,\, \pi)$, ξ_1 is a simple and unique eigenvalue that lie in the strip $0 < \mathcal{R}e(\xi_1) < \frac{\pi}{\omega_0}$.

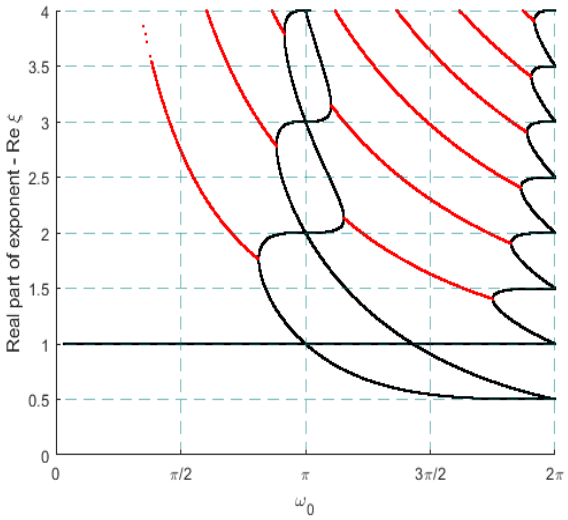

Figure 4: Distribution of the eigenvalues for SF-SF conditions.

Remarks 3.1. In consideration of Theorem 2.1, if someone wants to get a maximum regularity for the solution $\mathbf{u}$ of the problem (2.11), it is essential to reveal that the strip $\mathcal{R}e(\xi_\mu) \in (0, 2 - \frac{2}{p})$ is free of the root of the derived transcendental equations for various combinations of the boundary conditions.

So, for a closer look at the structure of distribution of the zeros of the equation (3.14) in a strip, the following proposition is described as follows.

Proposition 3.1. *If $\omega_0 \in (0, \pi)$, then the equation (3.14) has no root in the strip $\mathcal{R}e(\xi) \in (0, \frac{1}{2}]$ and If $\omega_0 \in (0, 2\pi)$, then this equation has no root in the strip $\mathcal{R}e(\xi) \in (0, \frac{1}{4}]$.*

Proof. The proposition is inspired by [7] and ([3], Remark A.7). We study the equation

$$\sin^2(\xi\omega_0) = m^2\xi^2 \sin^2(\omega_0), \tag{3.17}$$

with $m \in (0,1]$. It covers equation (3.14) by taking $m = 1$. It is noticeable that ξ is a solution of the equation (3.17) if and only if ξ satisfies the equations (3.18)-(3.19) below:

$$\sin(\xi\omega_0) = m\xi\sin(\omega_0), \tag{3.18}$$

$$\sin(\xi\omega_0) = -m\xi\sin(\omega_0). \tag{3.19}$$

We have to show that if $\omega_0 \in (0,\pi)$, then (3.18) has no root in the strip $\mathcal{R}e(\xi) \in (0,\frac{1}{2}]$. Similar argument displays the result of (3.19). Letting $\xi = a+ib$ with $a,b \in \mathbb{R}$ in (3.18) and separating the real and imaginary parts. Then the equation (3.18) is splits into two equations

$$\sin(a\omega_0)\cosh(b\omega_0) = ma\sin(\omega_0), \tag{3.20}$$

$$\cos(a\omega_0)\sinh(b\omega_0) = mb\sin(\omega_0). \tag{3.21}$$

Let us consider the two functions f_1, f_2 for a fixed $b \in \mathbb{R}$, such as

$$\begin{aligned} &f_1 : \mathbb{R} \to \mathbb{R} : a \to \sin(a\omega_0)\cosh(b\omega_0), \\ &f_2 : \mathbb{R} \to \mathbb{R} : a \to ma\sin(\omega_0). \end{aligned} \tag{3.22}$$

It is easily checked that

$$f_1(0) = f_2(0) = 0 \quad \text{and} \quad f_1(\frac{1}{2}) > f_2(\frac{1}{2}),$$

for $\omega_0 \in (0,\,\pi)$. Since, f_1 is concave in the interval $[0,\frac{\pi}{2\omega_0}]$, we get for all $a \in (0,\frac{1}{2}]$:

$$f_1(a) \geq 2af_1(\frac{1}{2}) > 2af_2(\frac{1}{2}) = f_2(a).$$

Therefore, for $\omega_0 \in (0,\,\pi)$, (3.20) does not coincide with (3.21) in the interval $(0,\frac{1}{2}]$. So does (3.18). Analogously, for $\omega_0 \in (0,\,2\pi)$ holds. □

The equation (3.17) recover the equation (3.13), since $m = \frac{1}{(3-4\nu)} \in (0,1]$.

Case 3: Hard clamped- Stress free boundary conditions (HC-SF)

$$D_{HC-SF}(\xi) = \xi^2\Big(\frac{1}{3-4\nu}\Big)\sin^2(\omega_0) - \frac{4(1-\nu)^2}{3-4\nu} + \sin^2(\xi\omega_0). \tag{3.23}$$

The numerical solutions to equation (3.23) are shown in Figures 5a-7 with $\mathcal{R}e(\xi) \in [0,4]$ and $\omega_0 \in (0,2\pi)$ with the same Poisson's ratios as given in Figures 1a-3, respectively. It is noticing that lower values of the Poisson's ratios implicate higher values of the threshold angle ω_0 with the singular terms. For instance, when $\nu = 0.5$ in plane strain conditions, the singular terms already arises for $\omega_0 > \frac{\pi}{4}$. Furthermore, for a certain angle ω_0 there may seem many singular terms of ξ real or complex contingent on Poisson's ratios. Such as, when $\omega_0 = \frac{3\pi}{2}$, and $\nu = 0.5$ (in plane strain), we have three real singular terms equivalent to three different values of $\xi \in (0,1)$, but if $\nu = 0.33$, two values of ξ, a real and complex one are found.

Proposition 3.2. *If $\omega_0 \in (0,\pi)$, then (3.23) has no root in the strip $\mathcal{R}e(\xi) \in (0,\frac{1}{2}]$. If $\omega_0 \in (0,2\pi)$, then this equation has no root in the strip $\mathcal{R}e(\xi) \in (0,\frac{1}{4}]$.*

Proof. Firstly, we have to show that the equation (3.23) has no root in the strip $\mathcal{R}e(\xi) \in (0, \frac{1}{2}]$ when $\omega_0 \in (0, \pi)$. Let we set $m_1 = \dfrac{1}{3-4\nu}$ and $m_2 = \dfrac{4(1-\nu)^2}{3-4\nu}$ in the equation (3.23). We let $\xi = a + ib$ with $a, b \in \mathbb{R}$ in (3.23) and separating the real and imaginary parts. Then the equation (3.23) can be split into the following two equations

$$\sin^2(a\omega_0)\cosh^2(b\omega_0) - \cos^2(a\omega_0)\sinh^2(b\omega_0) = m_2 - m_1(a^2 - b^2)\sin^2(\omega_0), \quad (3.24)$$

$$\sin(2a\omega_0)sinh(2b\omega_0) = -4m_1 ab\sin^2(\omega_0). \quad (3.25)$$

Now, we consider the two cases of the values of b.
Case I. If $b = 0$, then the equation (3.24) becomes

$$\sin^2(a\omega_0) = m_2 - m_1(a^2)\sin^2(\omega_0), \quad (3.26)$$

and has no solution $a \in [0, \frac{1}{2}]$. The direct computation gives us that the right hand-side is strictly greater than the left hand-side at $a = \frac{1}{2}$. Since, we get the result in the interval $[0, \frac{\pi}{2\omega_0}]$. Furthermore, the right hand-side of (3.26) is decreasing, while its left hand-side is increasing.
Case II. If $b \neq 0$, then a solution $a > 0$ of equation (3.25) satisfies

$$a > \frac{\pi}{2\omega_0} > \frac{1}{2}. \quad (3.27)$$

From (3.25), we find that

$$\frac{\sin(2a\omega_0)}{a} = \frac{-4bm_1\sin^2(\omega_0)}{sinh(2b\omega_0)}. \quad (3.28)$$

We get (3.27) since in the interval $a \in [0, \frac{\pi}{2\omega_0}]$. The right hand-side of (3.28) is always negative, while its left hand-side is positive.

By joining together the two cases, we get that (3.23) having no root in the strip $\mathcal{R}e(\xi) \in (0, \frac{1}{2}]$. Analogously, the case for $\omega_0 \in (0, 2\pi)$ can be proved. □

The similar propositions for the other cases of boundary conditions can be proved analogously to Propositions 3.1 and 3.2.

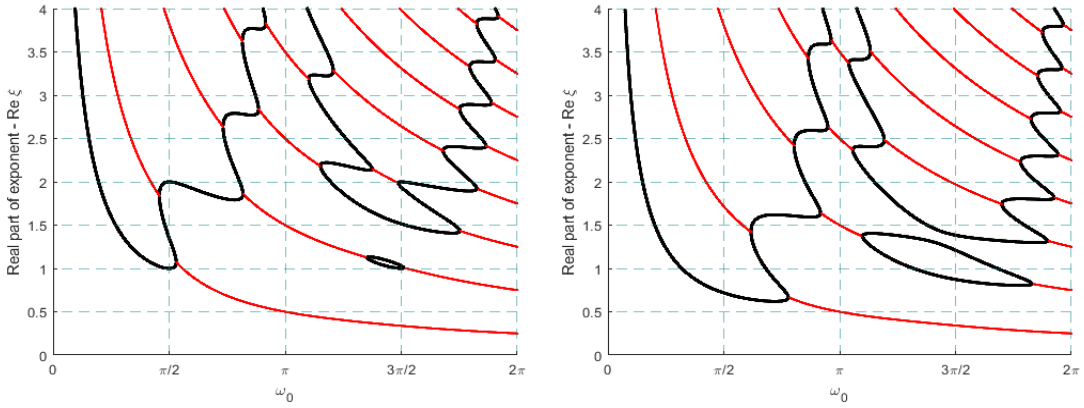

(a) Eigenvalues for HC-SF conditions for $\nu = 0.0$.

(b) Eigenvalues for HC-SF conditions for $\nu = 0.29$ (plane stress).

Figure 5: Distribution of the eigenvalues for HC-SF conditions for $\nu = 0.0$ and $\nu = 0.29$ (plane stress).

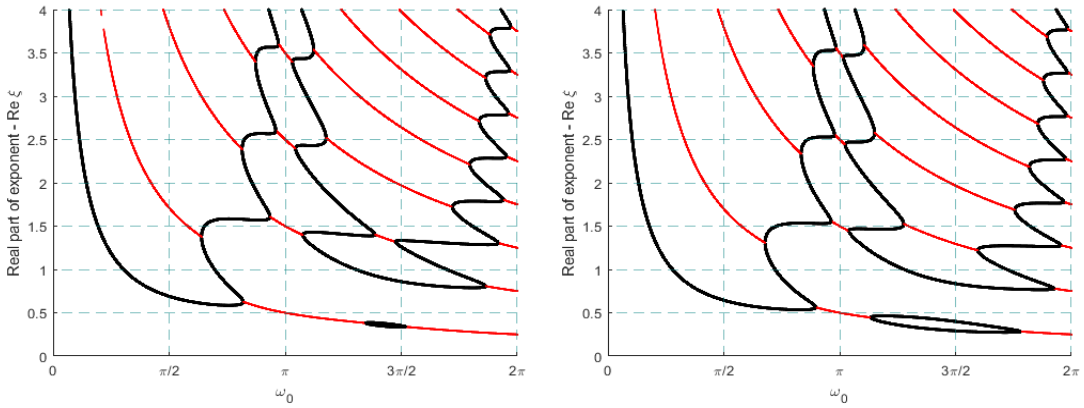

(a) Eigenvalues for HC-SF conditions for $\nu = 0.33$.

(b) Eigenvalues for HC-SF conditions for $\nu = 0.41$.

Figure 6: Distribution of the eigenvalues for HC-SF conditions for $\nu = 0.33$ and $\nu = 0.41$.

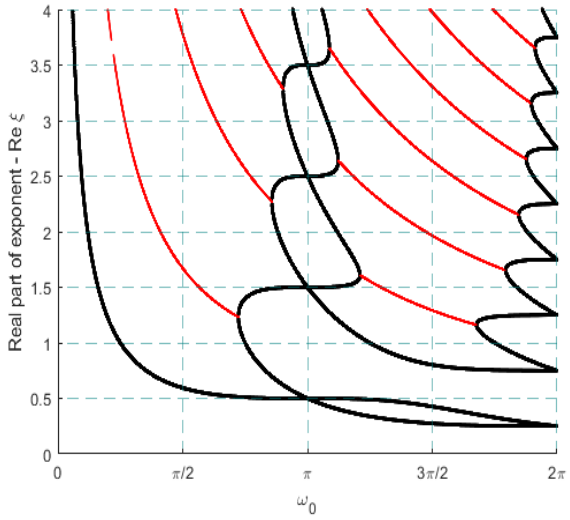

Figure 7: Distribution of the eigenvalues for HC-SF conditions for $\nu = 0.5$.

Case 4: Soft clamped- Soft clamped boundary conditions (SC-SC)
It means that the Soft clamped boundary conditions (2.5) are given on both sides of the angular corner point. Therefore, the computation leads to the transcendental equation

$$D_{SC-SC}(\xi) = \cos(2\xi\omega_0) - \cos(2\omega_0). \tag{3.29}$$

The roots of (3.29) are the eigenvalues of the operator $\hat{\mathcal{V}}_{SC-SC}(\xi) = \big[\hat{L}(\xi), \{\hat{B}_{[SC-SC]}(\xi)\}\big]$.

The distribution of zeros of equation (3.29) with $\mathcal{R}e(\xi) \in [0, 4]$ and $\omega_0 \in (0, 2\pi)$ is shown in Figure 8. We obtain the real eigenvalues ξ of (3.29) and can be given explicitly by

$$\xi_n = \pm\big(n\frac{\pi}{\omega_0} - 1\big), \tag{3.30}$$

where n is an integer.

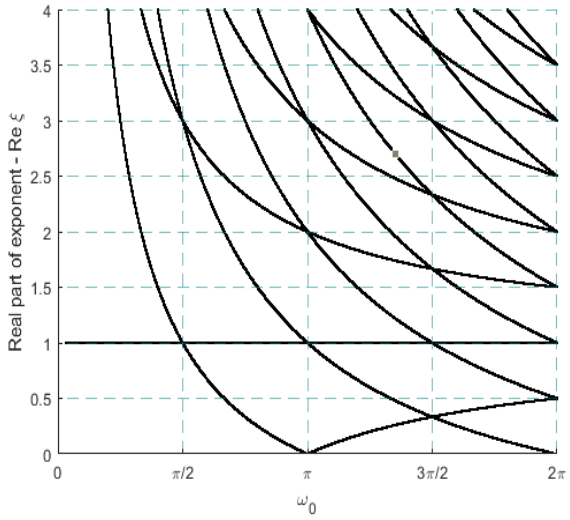

Figure 8: Distribution of the eigenvalues for SC-SC conditions.

Next, we only describe the characteristics equations of all the other possible combinations of the boundary conditions, whereas we give up the explicit specifications of the subsequent determinants.

Case 5: Hard clamped- Soft clamped boundary conditions (HC-SC)

$$D_{HC-SC}(\xi) = \sin(2\xi\omega_0) - \xi\Big(\frac{1}{3-4\nu}\Big)\sin(2\omega_0). \tag{3.31}$$

The numerical solutions to equation (3.31) for Poisson's ratios $\nu = 0.0, 0.29, 0.33, 0.41,$ and 0.5 are shown in Figures 9a-11 with $\mathcal{R}e(\xi) \in [0, 4]$ and $\omega_0 \in (0, 2\pi)$. It is noted that the singularity of the stress field arises for $\omega_0 > \frac{\pi}{2}$, for any value of the Poisson's ratios excepting $\nu = 0.5$ in Plane strain conditions, where the transient angle ω_0 jumps from $\frac{\pi}{2}$ to 0.7151π. Moreover, it is noted that for $\nu = 0.5$ in plane strain condition, equation (3.31) is the same as equation (3.36).

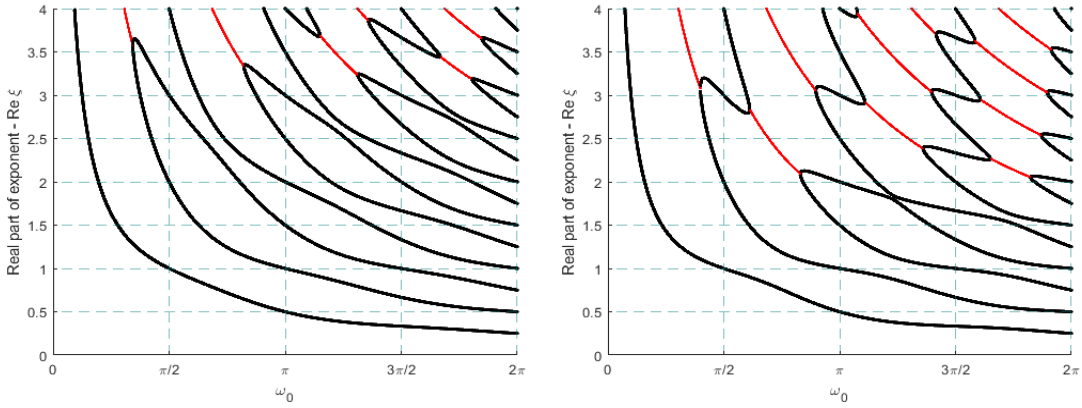

(a) Eigenvalues for HC-SC conditions for $\nu = 0.0$.

(b) Eigenvalues for HC-SC conditions for $\nu = 0.29$.

Figure 9: Distribution of the eigenvalues for HC-SC conditions for $\nu = 0.0$ and $\nu = 0.29$ (plane stress).

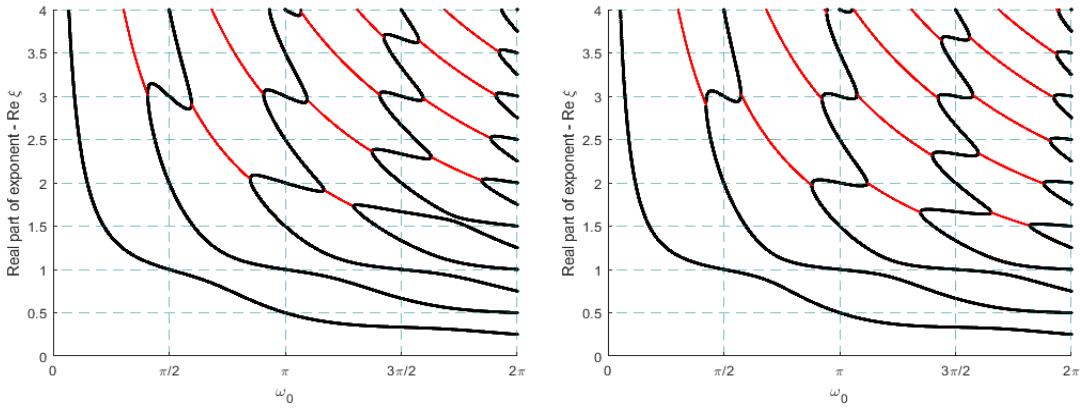

(a) Eigenvalues for HC-SC conditions for $\nu = 0.33$.

(b) Eigenvalues for HC-SC conditions for $\nu = 0.41$.

Figure 10: Distribution of the eigenvalues for HC-SC conditions for $\nu = 0.33$ and $\nu = 0.41$.

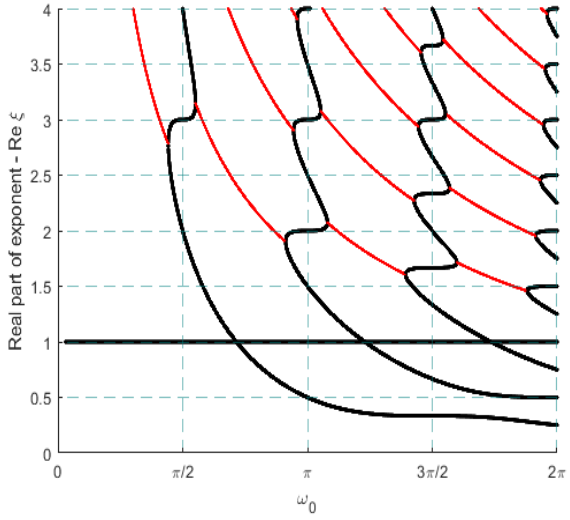

Figure 11: Distribution of the eigenvalues for HC-SC conditions for $\nu = 0.5$.

Case 6: Simply supported- Simply supported boundary conditions (SS-SS)

$$D_{SS-SS}(\alpha) = \cos^2(\xi\omega_0) - \cos^2(\omega_0). \tag{3.32}$$

The dispersal of zeros of equation (3.32) with $\mathcal{R}e(\xi) \in [0, 4]$ and $\omega_0 \in (0, 2\pi)$ is shown in Figure 12. It has the same eigenvalues corresponding to equation (3.30).

Case 7: Soft clamped- Simply supported boundary conditions (SC-SS)

$$D_{SC-SS}(\xi) = \cos(2\xi\omega_0) + \cos(2\omega_0). \tag{3.33}$$

The distribution of zeros of equation (3.33) with $\mathcal{R}e(\xi) \in [0, 4]$ and $\omega_0 \in (0, 2\pi)$ is shown in Figure 13. We obtain the real eigenvalues ξ of (3.33) and can be given explicitly by

$$\xi_n = \pm\Big[\big(\frac{1}{2} + n\big)\frac{\pi}{\omega_0} - 1\Big], \tag{3.34}$$

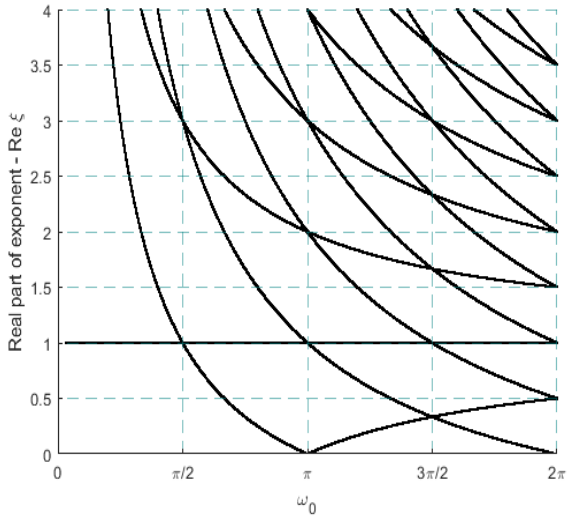

Figure 12: Distribution of the eigenvalues for SS-SS conditions.

where n is an integer.

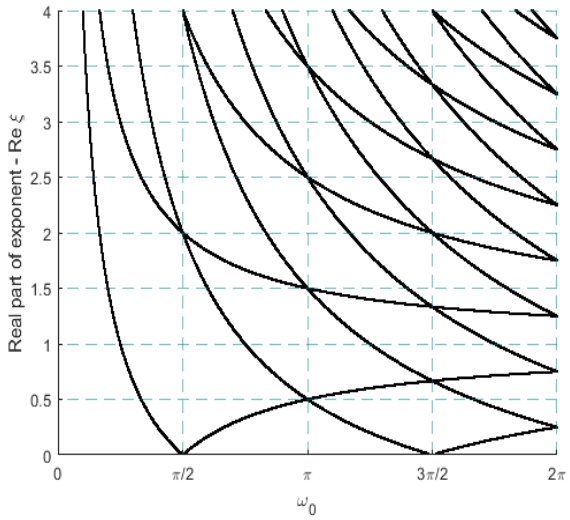

Figure 13: Distribution of the eigenvalues for SC-SS conditions.

Case 8: Hard clamped- Simply supported boundary conditions (HC-SS)

$$D_{HC-SS}(\xi) = \xi\Big(\frac{1}{3-4\nu}\Big)\sin(2\omega_0) + \sin(2\xi\omega_0). \tag{3.35}$$

The numerical solutions to equation (3.35) are shown in Figures 14a-16 with $\mathcal{R}e(\xi) \in [0, 4]$ and $\omega_0 \in (0, 2\pi)$ with the same Poisson's ratios as given in Figures 1a-3, respectively. The singular terms appear for $\omega_0 > \frac{\pi}{2}$.

It is noted that for $\nu = 0.5$ in plane strain condition, equation (3.35) is the same as the equation (3.37).

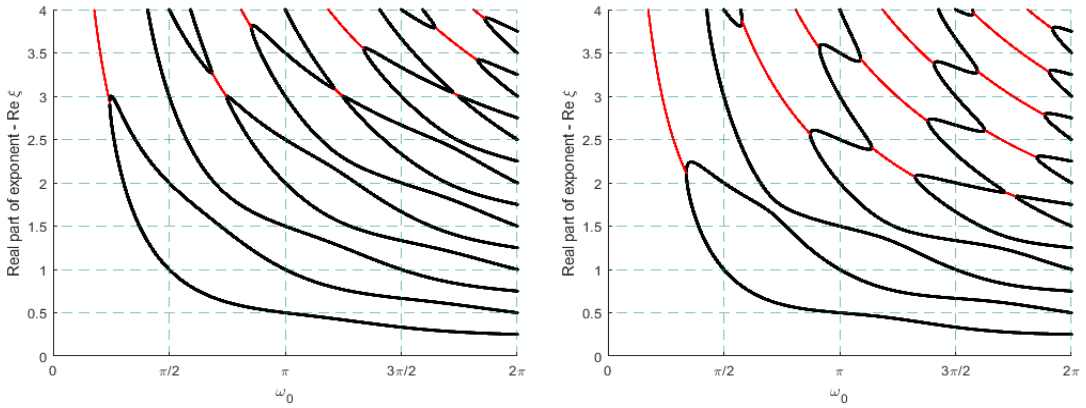

(a) Eigenvalues for HC-SS conditions for $\nu = 0.0$.

(b) Eigenvalues for HC-SS conditions for $\nu = 0.29$.

Figure 14: Distribution of the eigenvalues for HC-SS conditions for $\nu = 0.0$ and $\nu = 0.29$ (plane stress).

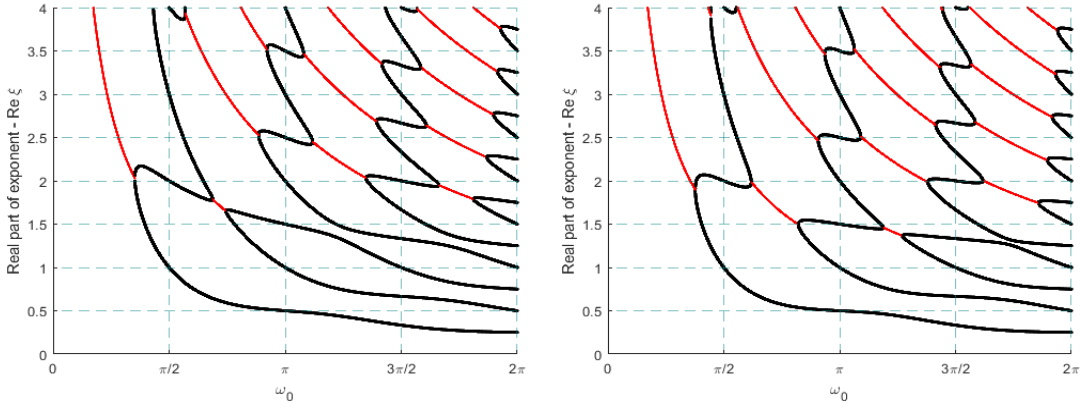

(a) Eigenvalues for HC-SS conditions for $\nu = 0.33$.

(b) Eigenvalues for HC-SS conditions for $\nu = 0.41$.

Figure 15: Distribution of the eigenvalues for HC-SS conditions for $\nu = 0.33$ and $\nu = 0.41$.

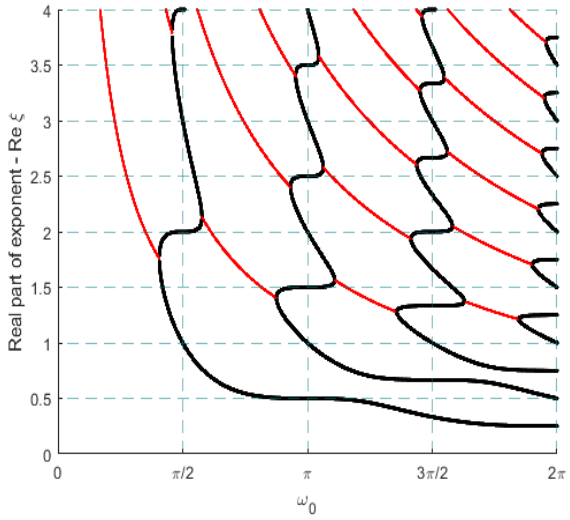

Figure 16: Distribution of the eigenvalues for HC-SS conditions for $\nu = 0.5$.

Case 9: Simply supported- Stress free boundary conditions (SS-SF)

$$D_{SS-SF}(\xi) = \sin(2\xi\omega_0) - \xi \sin(2\omega_0). \tag{3.36}$$

The numerical solutions to equation (3.36) are shown in Figure 17 with $\mathcal{R}e(\xi) \in [0, 4]$ and $\omega_0 \in (0, 2\pi)$. It is observed that the singularity of the stress field appears for $\omega_0 > 0.7151\pi$ and is defined by the real values of ξ. In the equations (3.14) and (3.36), $\xi = 1$ is always a zero of them. But this zero corresponds to a regular part of the solution, that is a rotation. So, we neglect $\xi = 1$ in the equivalent figures 4 and 17.

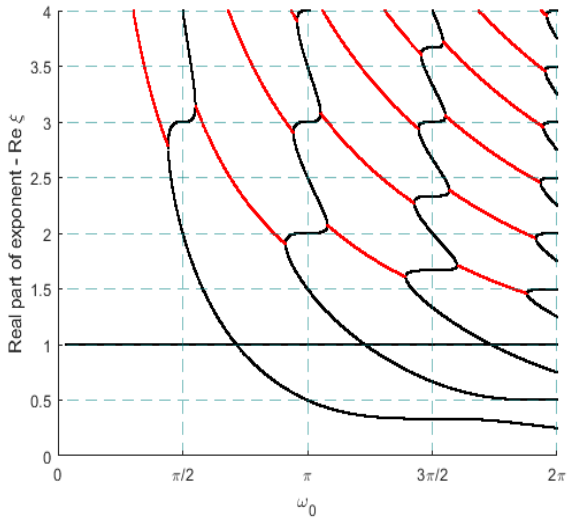

Figure 17: Distribution of the eigenvalues for SS-SF conditions.

Case 10: Soft clamped- Stress free boundary conditions (SC-SF)

$$D_{SC-SF}(\xi) = \sin(2\xi\omega_0) + \xi \sin(2\omega_0). \tag{3.37}$$

The numerical solutions to equation (3.37) are shown in Figure 18 with $\mathcal{R}e(\xi) \in [0, 4]$ and $\omega_0 \in (0, 2\pi)$. It is observed that the singularity of the stress field arises only for the real values of the exponents $\xi \left(\mathcal{R}e\left(\xi\right) \in (0, 1) \,\text{and}\, \text{Im}\left(\xi\right) = 0\right)$, which corresponds to $\omega_0 > \frac{\pi}{2}$.

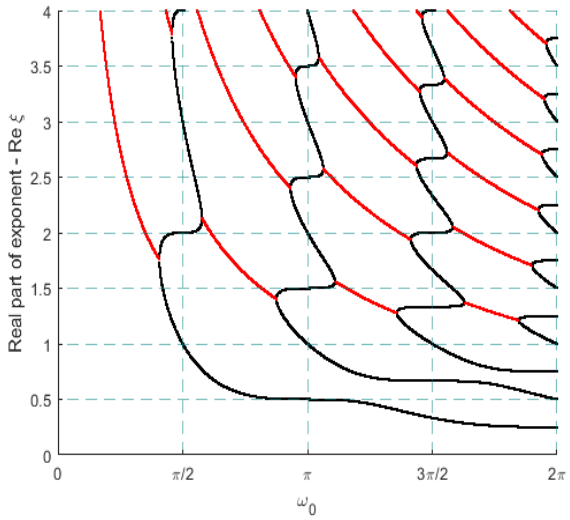

Figure 18: Distribution of the eigenvalues for SC-SF conditions.

3.2.1 Computation of the Singular Exponents

In section 3.2, we have completely discussed the distribution of the eigenvalues of the problem (2.8) for all the possible combinations of the boundary conditions. Now, we explain the process of computed these eigenvalues. As an example, we are considering the eigenvalue condition (3.14). The real eigenvalues of the eigenvalue condition (3.14) can be simply generated with MATLAB by an implicit plot, but it is much complicated to compute the complex eigenvalues. Here, we have developed the MATLAB program for the computation of the complex roots of the eigenvalue condition (3.14) (see appendix A), and the figure showing the distribution of the eigenvalues are given. We are interested only in those singularities in which the exponent lies in $0 \leq \mathcal{R}e\left(\xi_\mu\right) < 1$. The equation (3.14) is providing that an apex angle greater than π generates such exponents. The other eigenvalue conditions can be treated analogously.

Table 1 provides the representation of critical angles for stresses for various possible combinations of the boundary conditions.

Remarks 3.2. It is noted from the above-mentioned results that the qualitative properties of the solution including the regularity of the underlying problem depend on the properties of the singular exponents ξ_μ which are explicitly called the eigenvalues. It is observed that if $\mathcal{R}e\left(\xi_\mu\right) \geq 1$, then the solution defined in (2.14) is regular and belongs to space $W^{2,2}(\Omega)^2$. The case $\mathcal{R}e\left(\xi_\mu\right) = 0$ represents the translation which is regular. Hence, we consider only those eigenvalues of the generalized boundary eigenvalue problem that lies in the strip $0 \leq \mathcal{R}e\left(\xi_\mu\right) < 1$. Furthermore, the generalized eigenvalues depend on the values of the apex angle ω_0.

Table 1: Critical angles for the stresses for different boundary conditions

Boundary conditions	Angles	
HC-HC	π	
SF-SF	π	
SC-SC	$\pi/2$	
SS-SS	$\pi/2$	
HC-SC	$\pi/2$	For any Poisson ratio's $\nu = 0.0, 0.29, 0.33, 0.41$ except for $\nu = 0.5$ where the transient angle jumps from $\pi/2$ to $0.7151\,\pi$.
SC-SS	$\pi/4$	
SS-SF	$0.7151\,\pi$	
HC-SS	$\pi/2$	
HC-SF	$0.3422\,\pi$	For $\nu = 0.29$ (plain stress) and for $\nu = 0.5$ plain strain condition when the transient angle is $\pi/4$.
SC-SF	$\pi/2$	

4 Regularity Results

Let $\mathbf{u} \in \mathcal{U}(\Omega)$ be the unique weak solution of the boundary value problem (2.8). The understanding of the singular terms permits us to evaluate the maximal regularity of the weak solution. Based on Theorem 2.1 and the observations presented in Section 3, we describe the subsequent theorem.

Theorem 4.1. Let $\Omega \subset \mathbb{R}^2$ be a 2-dimensional bounded plane and connected domain. Suppose that the opening angle ω_0 at each of the angular boundary points P_i is lesser than the values given in Table 1. Then for any given data $\mathbf{f} \in L^2(\Omega)^2$, the weak solution $\mathbf{u}$ of the problem (2.8) has the regularity $\mathbf{u} \in \mathcal{U}(\Omega) \cap H^2(\Omega)$.

The regularity result for the elasticity problem in a polygonal domain for the characteristic equations (3.13), (3.14) and (3.23) are proved in [13, 22].

The following theorem gives the regularity of the solution of the problem (2.11) when all the ten possible combinations of the boundary conditions are applied on a domain Ω with angular corner points on the boundary.

Theorem 4.2. Let $\Omega \subset \mathbb{R}^2$ be a 2-dimensional bounded and connected domain with the interior angles ω_i at the angular corner points P_i of Γ. If Ω satisfies the following assumption that $\omega_i < 2\pi$ for all points P_i of the equations (3.13), (3.14), (3.23), (3.31), (3.35), (3.36), and (3.37), for $\omega_i < \frac{4}{5}\pi$ for all P_i of the equations (3.29) and (3.32), in addition to for $\omega_i < \frac{2}{5}\pi$ for all P_i of the equation (3.33). Then the solution $\mathbf{u}$ of the problem (2.11) for given data $\mathbf{f} \in L^2(\Omega)^2$ satisfies

$$\mathbf{u} \in H^{\frac{5}{4}+\delta}(\Omega)^2, \text{ for some } \delta > 0. \tag{4.1}$$

Proof. For the proof, we proceed as [Section 1.4.5, 14]. By the assumption on the domain Ω and the descriptions regarding the distribution of zeros of the derived transcendental

equations specified in Section 3, that the strip $\mathcal{R}e(\xi) \in (0, \frac{1}{4}]$ is free of the root for all possible cases of the combination of the boundary conditions at each point P_i of the boundary Γ. Additionally, it is recognized that in a fixed strip $\mathcal{R}e(\xi) \in [m, n]$ with $m, n \in \mathbb{R}$, the obtained characteristic equations (3.13), (3.14), (3.23),(3.29), (3.31)-(3.33), and (3.35)-(3.37) have only a finite number of isolated roots, therefore there exists a $p \in \left]\frac{8}{7}, 2\right[$, such that at each point of Γ the strip $\mathcal{R}e(\xi) \in \left(0, 2 - \frac{2}{p}\right]$ is free of the root. In consequence of Theorem 2.1, we conclude that the solution $\mathbf{u}$ of the considered problem belongs to $W^{2,p}(\Omega)^2$ for such a p. Using [Theorem 1.4.4.1, 14], we get (4.1), since the domain Ω has a Lipschitz boundary. □

Remarks 4.1. It is noted that if the domain Ω satisfies the assumptions of Theorem 4.2, then for $\omega_i < 2\pi$ for all points P_i of the equations (3.13)and (3.14), for $\omega_i < \pi$ for all P_i of (3.31), (3.35), (3.23), (3.37) and (3.36), for $\omega_i < \frac{2}{3}\pi$ for all P_i of (3.29) and (3.32), in addition to $\omega_i < \frac{\pi}{3}$ for all P_i of (3.33), then the solution $\mathbf{u}$ of the problem (2.11) for given data $\mathbf{f} \in L^2(\Omega)^2$ satisfies $\mathbf{u} \in H^{\frac{3}{2}+\delta}(\Omega)^2$, for some $\delta > 0$.

5 Conclusion

In this paper, a mathematically rigorous description of the corner singularities of the weak solutions for the plane linearized elasticity system in a bounded planar domain with angular corner points on the boundary has been given. To analyze the behavior of solutions of the considered problem in the vicinity of the singularities, we have extended our analysis by considering all ten possible cases of combinations of the boundary conditions generated by the basic four ones in classical elasticity [2, 19] proposing in the two natural directions of the boundary, i.e., tangential and normal direction, respectively, which have not yet studied. In particular, the resulting expansion involves singular vector functions, inlines, depending on a certain parameter ξ_μ. Since they generate the singular functions as a power of r. The transcendental equations illustrating the corner singularity exponents for these combinations of the boundary conditions have been derived with the aid of the determinant method. Analytically, it was much difficult to determine the values of a parameter ξ_μ from these transcendental equations. Consequently, a MATLAB program has been developed (see appendix A), whereby the parameter ξ_μ has been computed, and figures showing their distributions have been presented. Moreover, we have computed the leading singular exponents for all these combinations of the boundary conditions, wherein the critical angles $\omega_{critical}$ have been listed in Table 1 such that for interior angles $\omega < \omega_{critical}$ the H^2-regularity of solution can be guaranteed.

Additionally, it has been observed that if $\mathcal{R}e\,(\xi_\mu) \geq 1$, then the solution of the underlying problem is regular and belongs to $W^{2,2}(\Omega)^2$. The case $\mathcal{R}e\,(\xi_\mu) = 0$ represents the translation which is regular. The terms with $\mathcal{R}e\,(\xi_\mu) < 1$ are called the singular terms since they yield the unbounded stresses. So, we have considered only those eigenvalues of the boundary eigenvalue problem that lies in the strip $0 \leq \mathcal{R}e\,(\xi_\mu) < 1$ which in turn depends on the angles ω. The characterization of stress singularities for these combinations of the boundary conditions in terms of the inner angle of a corner point has been studied. Finally, it has been proved that the solution $\mathbf{u}$ of the considered problem belongs to $W^{2,p}(\Omega)^2$ for all the possible cases of the combinations of the boundary conditions at each point P_i of the Γ, when the strip $\mathcal{R}e(\xi) \in \left(0, 2 - \frac{2}{p}\right]$ is free of the root for such a p which belongs to $\left]\frac{8}{7}, 2\right[$.

Conflict of interest

The authors declares that no conflict of interest exists.

References

[1] T. L. Anderson. Fracture Mechanics: Fundamentals and Applications. Vol. Fourth Edition. CRC Press, 2017.

[2] R. J. Atkin and N. Fox. An introduction to the theory of elasticity. Dover Publications, 2013.

[3] M. Beneš and P. Kučera. Solutions to the Navier-Stokes equations with mixed boundary conditions in two-dimensional bounded domains. *Mathematische Nachrichten.* 289(2-3) (2015), 194–212.

[4] F. Berto, L. P. Pook, and A. Campagnolo. Corner point singularities under in-plane and out-of-plane loading: a review of recent results. *Engineering Solid Mechanics* (2017), 167–176.

[5] W. Booncharoen, Y. Sompornjaroensuk, and P. Kongtong. A revisit to the Williams's solution in bending problem of plates with stress singularities. *International Journal of Mathematical Analysis.* 7 (2013), 1301–1316.

[6] R. M. Brown and I. Mitrea. The mixed problem for the Lamé system in a class of Lipschitz domains. *Journal of Differential Equations.* 246(7) (2009), 2577–2589.

[7] M. Dauge. Stationary Stokes and Navier–Stokes systems on two- or three-dimensional domains with corners. part I. linearized equations. *SIAM Journal on Mathematical Analysis.* 20(1) (1989), 74–97.

[8] M. Dauge. Elliptic boundary value problems on corner domains: smoothness and asymptotics of solutions. Vol. 1341. 2006.

[9] M. Dauge, I. Gruais, and A. RÃ¶ssle. The influence of lateral boundary conditions on the asymptotics in thin elastic plates. *SIAM Journal on Mathematical Analysis.* 31(2) (2000), 305–345.

[10] J. P. Dempsey and G. B. Sinclair. On the singular behavior at the vertex of a bi-material wedge. *Journal of Elasticity. The Physical and Mathematical Science of Solids.* 11(3) (1981), 317–327.

[11] A. H. England. On stress singularities in linear elasticity. *International Journal of Engineering Science.* 9(6) (1971), 571–585.

[12] A. S. Gjam, H. A. Abdusalam, and A. F. Ghaleb. Solution for a problem of linear plane elasticity with mixed boundary conditions on an ellipse by the method of boundary integrals. *Journal of the Egyptian Mathematical Society.* 21(3) (2013), 361–369.

[13] P. Grisvard. Singularité s en elasticité. *Archive for Rational Mechanics and Analysis.* 107(2) (1989), 157–180.

[14] P. Grisvard. Elliptic problems in nonsmooth domains. Vol. 2, 2–2. pitman advanced pub. Program, Boston, 1985.

[15] V. L. Hein and F. Erdogan. Stress singularities in a two-material wedge. *International Journal of Fracture Mechanics.* 7(3) (1971).

[16] A. Kotousov and Y. T. Lew. Stress singularities resulting from various boundary conditions in angular corners of plates of arbitrary thickness in extension. *International Journal of Solids and Structures*. 43(17) (2006), 5100–5109.

[17] V. Kozlov, V. Maz'ya, and J. Rossmann. Elliptic boundary value problems in domains with point singularities. American Mathematical Society, 1997.

[18] V. Kozlov, V. Maz'ya, and J. Rossmann. Spectral problems associated with corner singularities of solutions to elliptic equations. Vol. 85. 2001.

[19] V. D. Kupradze, T. G. Gegelia, M. O. Basheleĭshvili, and T. V. Burchuladze. Three-dimensional problems of the mathematical theory of elasticity and thermoelasticity. Vol. 25. North-Holland Series in Applied Mathematics and Mechanics. North-Holland Publishing Co., Amsterdam-New York, 1979, 929.

[20] H. Li and J. Huang. Solution of two-dimensional elasticity problems using a high-accuracy boundary element method. *Applied Numerical Mathematics*. 161 (2021), 52–68.

[21] A. L. Mazzucato and V. Nistor. Well-posedness and regularity for the elasticity equation with mixed boundary conditions on polyhedral domains and domains with cracks. *Archive for Rational Mechanics and Analysis*. 195(1) (2010), 25–73.

[22] S. Nicaise. About the Lamé system in a polygonal or a polyhedral domain and a coupled problem between the Lamé system and the plate equation. I: Regularity of the solutions. *Annali della Scuola Normale Superiore di Pisa-Classe di Scienze*. 19(3) (1992), 327–361.

[23] K. A. Ott and R. M. Brown. The mixed problem for the Lam'e system in two dimensions. *Journal of Differential Equations*. 254(12) (2013), 4373–4400.

[24] L. P. Pook, F. Berto, and A. Campagnolo. State of the art of corner point singularities under in-plane and out-of-plane loading. *Engineering Fracture Mechanics*. 174 (2017), 2–9.

[25] A. Rössle and A.-M. Sändig. Corner singularities and regularity results for the Reissner/Mindlin plate model. *Journal of Elasticity. The Physical and Mathematical Science of Solids*. 103(2) (2011), 113–135.

[26] A.-M. Sändig, U. Richter, and R. Sändig. The regularity of boundary value problems for the Lamé equations in a polygonal domain. *Rostocker Mathematisches Kolloquium*. (36) (1989), 21–50.

[27] A. Seweryn and K. Molski. Elastic stress singularities and corresponding generalized stress intensity factors for angular corners under various boundary conditions. *Engineering Fracture Mechanics*. 55(4) (1996), 529–556.

[28] G. B. Sinclair. Logarithmic stress singularities resulting from various boundary conditions in angular corners of plates in extension. *American Society of Mechanical Engineers. Transactions of the ASME. Journal of Applied Mechanics*. 66(2) (1999), 556–560.

[29] G. B. Sinclair. Stress singularities in classical elasticity-II: Asymptotic identification. *Applied Mechanics Reviews*. 57(5) (2004), 385–439.

[30] J. J. Tripathi, G. D. Kedar, and K. C. Deshmukh. Generalized thermoelastic diffusion in a thick circular plate including heat source. *Alexandria Engineering Journal*. 55(3) (2016), 2241–2249.

[31] V. V. Vasil'ev and S. A. Lurie. Generalized theory of elasticity. *Mechanics of Solids*. 50(4) (2015), 379–388.

[32] H. Volkmer. Eigenvalue problems for Lamé's differential equation. *SIGMA. Symmetry, Integrability and Geometry. Methods and Applications*. 14(131) (2018), 21.

[33] M. L. Williams. Stress singularities resulting from various boundary conditions in angular corners of plates in extension. *Journal of Applied Mechanics*. 19(4) (1952), 526–528.

[34] Z. Yosibash. Singularities in elliptic boundary value problems and elasticity and their connection with failure initiation. Springer New York, 2012.

A Appendix

MATLAB program for the computation of real eigenvalues of the eigenvalue condition

```
% Program that compute the real roots
% of the eigenvalue conditions and plot them.
function [] = root_ploting(omega_start,omega_end,q)
% Function [] = root_ploting(q)

% Description
% The function compute the real root of the complex number
% in the given area using angle w0.
%
% Input:
% q: Eigenvalue conditions as an inline function based on
%    lambda and w0. Where lambda = a + i*b
% Output:
% output:  output(i)*real
iota = sqrt(-1);
syms lambda omega0;
%input function q, starting and ending value of omega
%output: plotting of real roots of q between omega
q = (lambda).^2.*sin(omega0).^2-sin(lambda*omega0).^2;
omega_start = 0;
omega_end = 2*pi;
% f = matlabFunction(q,'Vars',[lambda,omega0]) generates a
    MATLAB
% anonymous function
f =  matlabFunction(q,'Vars',[lambda,omega0]);
df = matlabFunction(diff(f(lambda,omega0),lambda));
% If maximum 10 points satisfy the accuracy
% refine the decimal power
omega0_refiner = 100;
omega0 = (omega_start:.1/omega0_refiner:omega_end)';
nomega0 = length(omega0);
```

```
% Change ymax to adjust the vertical range of plot
ymax = 4;
% Change the value of initial guess refiner for finer selction
    of initial
% guess
initial_guess_refiner = 2;
r = 0:.01/initial_guess_refiner:ymax;
nr = length(r);
% iter represent the total number of iterations and tol
    represent
% tolerance
iter = 10;
tol = 1.0e-10;
figure(1)
hold on;
% Loop over area of the angle
% Program should be able to compute the root as area of angle
    top down
for j=1:nr
    z = r(j)+rand*iota;
    for k=1:iter
        z = z-f(z,omega0)./df(z,omega0);
        norm_f = abs(f(z,omega0));
    end
    idata = [];
    for i=1:nomega0
        if(norm_f(i)<tol)
            idata = [idata;i];
            disp('success');
        end
    end
% Xticks returns a vector containing the x-axis tick
% values for the current axes.
xticks([0 pi/2 pi 3*pi/2 2*pi ])
xticklabels({'0', '\pi/2', '\pi', '3\pi/2', '2\pi'})
xlabel('\omega_{0}')
ylabel('Real \xi')
title('Graphs of the Real Roots of the Eigenvalue Conditions')
grid
% axes specified by ax instead of the current axes.
ax = gca;
ax.GridColor = [0 .5 .5];
ax.GridLineStyle = '--';
ax.GridAlpha = 0.5;
ax.Layer = 'top';

    omega0i = omega0(idata);
    zi  = z(idata);
    cond1 =abs(imag(zi))<.0001;
```

```
77      cond2 =abs(imag(zi))>=.0001;
78      cond3 =abs(real(zi))>=.01;
79      ind1 = find(cond1 & cond3);
80      ind2 = find(cond2 & cond3);
81  % Plot the imaginary and real regions
82      plot(omega0i(ind1),real(zi(ind1)),'.k','MarkerSize',6);
83      plot(omega0i(ind2),real(zi(ind2)),'.r','MarkerSize',2);
84      axis([0 2*pi 0 4])
85      drawnow;
86  end
87
88  end
```